DOI: 10.1002/ejic.200800296

Two Hexanickel-Substituted Keggin-Type Germanotungstates[‡]

Jun-Wei Zhao,[a] Jie Zhang,[a] You Song,[b] Shou-Tian Zheng,[a] and Guo-Yu Yang*[a]

Keywords: Polyoxometalates / Hydrothermal synthesis / Nickel / Amines

Two new inorganic–organic hybrid germanotungstates built from trivacant Keggin fragments and in situ generated hexanickel clusters $[Ni(en)_2]_{0.5}[\{Ni_6(\mu_3\text{-}OH)_3(en)_3(H_2O)_6\}(B\text{-}\alpha\text{-}GeW_9O_{34})]\cdot 3H_2O$ (**1**) and $[\{Ni_6(\mu_3\text{-}OH)_3(dap)_3(H_2O)_6\}(B\text{-}\alpha\text{-}GeW_9O_{34})]\cdot H_3O\cdot 4H_2O$ (**2**) (en = ethylenediamine and dap = 1,2-diaminopropane) were hydrothermally synthesized and characterized by IR spectroscopy, elemental analysis, thermogravimetric analysis, single-crystal X-ray diffraction and magnetic analysis. Compound **1** crystallizes in the monoclinic space group $P2_1/n$; whereas compound **2** crystallizes in the monoclinic space group $P2_1/c$. Single-crystal X-ray diffraction indicates that both contain a hexa-Ni^{II}-substituted trivacant Keggin unit $[\{Ni_6(\mu_3\text{-}OH)_3(L)_3(H_2O)_6\}(B\text{-}\alpha\text{-}GeW_9O_{34})]^-$ (L = en or dap). Magnetic susceptibility measurements show the presence of ferromagnetic coupling interactions within the hexa-Ni^{II} clusters for **1** and **2**.

Introduction

Polyoxometalates (POMs) are a unique class of metal–oxygen cluster species with a diverse compositional range, an enormous structural variety and extensive electronic versatility.[1,2] Although POM chemistry has a long history of almost two centuries, hitherto, most of the work is still focused on making and characterizing inorganic lacunary POM derivatives usually by conventional aqueous solution methods.[3] Moreover, the mechanisms of formation are not well understood and are commonly described as self assembly. As a result, the systematic design and synthesis of novel POM species with unexpected structures and properties remain a continuous challenge for profound progress in POM chemistry.

In recent years, the chemistry of d-electron transition-metal-substituted polyoxometalates (TMSPs) have attracted increasing interests owing to possible applications involving redox- and acid-dependent catalysis, molecular magnetism and medicine as well as their highly tuneable nature and intrinsic structural characteristics.[1,4] The progress of TMSP chemistry is principally driven by the synthesis and characterization of new compounds possessing unique topologies and performances. One of the most useful synthetic strategies incorporates a large number of paramagnetic transition-metal (TM) ions or clusters into the frameworks of lacunary polyoxoanion segments to obtain the targeted TMSP species with various stoichiometries and structural features combined with interesting magnetic and catalytic properties.[5] Moreover, lacunary polyoxoanion fragments have been proven to be versatile inorganic functional ligands used to construct high-nuclear magnetic clusters. In the past several decades, a multitude of lacunary polyoxoanions have been functionalized by TM cations directly resulting in the largest pure inorganic sandwich-type subclass,[6] where the number of TM cations among reported examples is usually less than six. The Ni^{II}-substituted TMSPs are a large family of important POM clusters, because the ferromagnetic spin couplings between Ni^{II} ions can lead to material intermediates.[7] These reported Ni^{II}-substituted TMSPs can be subdivided into two types: sandwich type and nonsandwich type. On one hand, the sandwich type is represented by two lacunary POM fragments linked by two to seven Ni^{II} cores. For example, in 1994, Coronade et al. reported a α-Dawson-based sandwich-type phosphotungstate $[Ni_4(H_2O)_2(\alpha\text{-}P_2W_{15}O_{56})_2]^{16-}$ incorporating a ferromagnetic Ni^{II} tetramer,[8] and subsequently, he reported a tetra-Ni^{II} sandwiched α-Keggin-based phosphotungstate $[Ni_4(H_2O)_2(B\text{-}\alpha\text{-}PW_9O_{34})_2]^{10-}$ in 1999.[3f] Kortz et al. communicated a novel di-Ni^{II}-substituted β-Keggin-type silicotungstate $[\{\beta\text{-}SiNi_2W_{10}O_{36}(OH)_2(H_2O)\}_2]^{12-}$ in 1999.[7c] Wang et al. described a tetra-Ni^{II} sandwiched Dawson-type arsenic analogue $[Ni_4(H_2O)_2(\alpha\text{-}As_2W_{15}O_{56})_2]^{16-}$ in 2000.[9] Later, Kortz et al. addressed a tri-Ni^{II}-substituted sandwich-type phosphotungstate $[Ni_3Na(H_2O)_2(B\text{-}\alpha\text{-}PW_9O_{34})_2]^{11-}$.[10] In 2006, Wang et al. synthesized two hexa- or hepta-Ni^{II} substituted polyoxotungstates (POTs): $[\{Ni_6(H_2O)_4(\mu_2\text{-}H_2O)_4(\mu_3\text{-}OH)_2\}(SiW_9O_{34})_2]^{10-}$

[‡] Combination of Lacunary Polyoxometalates and High-Nuclear Transition-Metal Clusters under Hydrothermal Conditions, VI. Part V: J.-W. Zhao, J. Zhang, S.-T. Zheng, G.-Y. Yang, *Inorg. Chem.* **2007**, *46*, 10944–10846.

[a] State Key Laboratory of Structural Chemistry, Fujian Institute of Research on the Structure of Matter and Graduate School of Chinese Academy of Sciences
Fuzhou, Fujian 350002, China
Fax: +86-591-8371-0051
E-mail: ygy@fjirsm.ac.cn
[b] State Key Laboratory of Coordination Chemistry, School of Chemistry and Chemical Engineering, Nanjing University
Naning, Jiangsu 210093, China

and $[Ni_7(OH)_4(H_2O)(CO_3)_2(HCO_3)(A\text{-}\alpha\text{-}SiW_9O_{34})(\beta\text{-}SiW_{10}O_{37})]^{10-}$.[3h] On the other hand, the nonsandwich type is represented by a monomeric tetra-Ni^{II}-cubane-substituted Keggin POT $[H_2PW_9Ni_4(OH)_3(H_2O)_6]^{2-}$[11] and a related monotungsten-capped POT $[Ni_3(H_2O)_3PW_{10}O_{39}(H_2O)]^{7-}$.[3f] A novel banana-shaped polyoxoanion $[Ni_6As_3W_{24}O_{94}(H_2O)_2]^{17-}$ was documented in 2003, which consists of two $[B\text{-}\alpha\text{-}Ni_3AsW_9O_{40}]^{15-}$ Keggin moieties linked through a $[AsW_6O_{16}]^{9+}$ fragment.[5] Another trimeric POT $[Ni_9(OH)_3(H_2O)_6(HPO_4)_2(B\text{-}\alpha\text{-}PW_9O_{34})_3]^{16-}$ was also reported, which contains a nona-Ni^{II} cluster encapsulated in three trivacant Keggin fragments.[3f] Recently, the investigation on Ni^{II}-containing TMSPs demonstrated the electrocatalytic reduction of nitrates in mildly acidic aqueous media and the catalytic effect was found to increase with the number of nickel centres.[12] Additionally, although many inorganic–organic hybrid (4–9)-nuclear nickel^{II} clusters have been found in coordination chemistry,[13] the inorganic–organic hybrid system based on lacunary POM precursors and Ni^{II} complex cations remains less explored under hydrothermal conditions.[14] Hence, we believe that the effective combination of lacunary POM precursors and Ni^{II} complex cations with hydrothermal techniques will open a new avenue in making novel high-nuclear TMSP clusters with interesting magnetic or other properties. Recently, we developed an effective strategy that involves the use of lacunary sites of polyoxoanion fragments as structure-directing agents (SDAs) to induce high-nuclear TM clusters and multidentate N ligands as structure-stabilizing agents (SSAs). These SSAs are then used to capture and stabilize in situ generated TM clusters to construct novel magnetic POT oligomers or aggregates under hydrothermal conditions.[14] In this way, we obtained a class of novel-inorganic–organic hybrid POTs $[NiL_2]_m[\{Ni_6(\mu_3\text{-}OH)_3L_{3-n}(H_2O)_{6+2n}\}(B\text{-}\alpha\text{-}XW_9O_{34})]\cdot yH_2O$ (L = diamines, X = P^V/Si^{IV}) and $[\{Ni_7(\mu_3\text{-}OH)_3O_2(dap)_3(H_2O)_6\}(B\text{-}\alpha\text{-}PW_9O_{34})][\{Ni_6(\mu_3\text{-}OH)_3(dap)_3(H_2O)_6\}(B\text{-}\alpha\text{-}PW_9O_{34})][Ni(dap)_2(H_2O)_2]\cdot 4.5H_2O$ based on a single trivacant Keggin fragment capped by a hexa-Ni^{II} or hepta-Ni^{II} unit.[14a,14b] Moreover, we also obtained a family of inorganic–organic hybrid tetra-Ni^{II} sandwiched POTs with discrete or 2D structures.[14c,14d] For instance, three rare inorganic–organic hybrid 2D nets constructed from tetra-Ni^{II} sandwiched units $\{[Ni(dap)_2(H_2O)]_2[Ni(dap)_2]_2[Ni_4(Hdap)_2(B\text{-}\alpha\text{-}HXW_9O_{34})_2]\}$ (n = 1, X = Si^{IV}, Ge^{IV}; n = 0, X = P^V) as building blocks were synthesized by us.[14c] In addition, two novel hexa-Cu^{II}-substituted POTs $[Cu_6(\mu_3\text{-}OH)_3(en)_3(H_2O)_3(B\text{-}\alpha\text{-}PW_9O_{34})]\cdot 7H_2O$[14b] and $[Cu(dap)_2]_2\{[Cu(dap)_2(H_2O)]_2[Cu_6(dap)_2(B\text{-}\alpha\text{-}SiW_9O_{34})_2]\}\cdot 4H_2O$[15] were also isolated. Furthermore, two unprecedented octa-Cu^{II} sandwiched POTs $[Cu(dap)(H_2O)_3]_2[\{Cu_8(dap)_4(H_2O)_2\}(B\text{-}\alpha\text{-}SiW_9O_{34})_2]\cdot 6H_2O$ and $[Cu(H_2O)_2]H_2[Cu_8(dap)_4(H_2O)_2(B\text{-}\alpha\text{-}GeW_9O_{34})_2]$ were separated in our lab.[14b,16] As a continuance of our recent work, herein, we report the syntheses, crystal structures and magnetic properties of two new inorganic–organic hybrid germanotungstates built from trivacant Keggin fragments and in situ generated hexanickel cluster units $[Ni(en)_2]_{0.5}[\{Ni_6(\mu_3\text{-}OH)_3(en)_3(H_2O)_6\}(B\text{-}\alpha\text{-}GeW_9O_{34})]\cdot 3H_2O$ (**1**) and $[\{Ni_6(\mu_3\text{-}OH)_3(dap)_3(H_2O)_6\}(B\text{-}\alpha\text{-}GeW_9O_{34})]\cdot H_3O\cdot 4H_2O$ (**2**) (en = ethylenediamine and dap = 1, 2-diaminopropane). Structural analyses indicate that both compounds contain a hexanickel-substituted trivacant Keggin POM unit $[\{Ni_6(\mu_3\text{-}OH)_3L_3(H_2O)_6\}(B\text{-}\alpha\text{-}GeW_9O_{34})]^-$ (L = en or dap). Magnetic susceptibility measurements show the presence of ferromagnetic coupling interactions within the hexa-Ni^{II} clusters with J_1 = 0.68 cm^{-1}, J_2 = 1.48 cm^{-1} for **1** and J_1 = 0.67 cm^{-1}, J_2 = 1.52 cm^{-1} for **2**.

Results and Discussion

Synthesis

Many pure inorganic TMSPs can be easily obtained on the basis of mono- di-, tri- and multilacunary POM precursors by virtue of the conventional aqueous solution method, especially for Keggin- and Dawson-type POTs. However, this routine method is not suitable for the preparation of inorganic–organic hybrid hexa-Ni^{II}-substituted trivacant Keggin POTs in the presence of organoamines (e.g., dap or en), partly because Ni^{II} ions, lacunary POM precursors and organoamines cannot be completely dissolved in aqueous systems at the same time; therefore, we employed the hydrothermal method, which is an effective method for growing crystals of numerous hybrid materials.[17a–17d] As we know, the rational design of an experiment needs two steps: the first is to identify the structural type and probable chemical compositions that would give rise to the desired properties, and the second step is to find an appropriate method to make the materials.[17e] Although we are far from the ultimate dream of "tailor making" desired products with specified structures and properties, the rational design has been possible to a limited extent within selected families of compounds. In our case, it may be possible to predict the existence of new phases within the same structural types by analogy to already known phases.

In our experiment, a hexa-Ni^{II}-substituted phosphotungstate $[\{Ni_6(\mu_3\text{-}OH)_3(en)_3(H_2O)_6\}(B\text{-}\alpha\text{-}PW_9O_{34})]\cdot 7H_2O$ (**3**) (Table 1) was initially isolated by reaction of $Na_9[A\text{-}\alpha\text{-}PW_9O_{34}]\cdot 7H_2O$ with $NiCl_2\cdot 6H_2O$ in the presence of en.[14b] By enlightenment of this compound, we consecutively isolated seven analogous species: $[\{Ni_6(\mu_3\text{-}OH)_3(en)_2(H_2O)_8\}(B\text{-}\alpha\text{-}PW_9O_{34})]\cdot 7H_2O$ (**4**),[14b] $[\{Ni_6(\mu_3\text{-}OH)_3(dap)_2(H_2O)_8\}(B\text{-}\alpha\text{-}PW_9O_{34})]\cdot 7H_2O$(**5**),[14b] $[Ni(dap)_2(H_2O)_2][Ni_6(\mu_3\text{-}OH)_3(H_2O)_4(dap)_3(CH_3COO)(B\text{-}\alpha\text{-}PW_9O_{34})]_2\cdot 10H_2O$ (**6**),[14a] $[Ni_6(\mu_3\text{-}OH)_3(H_2O)_2(dien)_3(B\text{-}\alpha\text{-}PW_9O_{34})]\cdot 4H_2O$ (**7**),[14a] $[\{Ni_6(\mu_3\text{-}OH)_3(en)_3(H_2O)_6\}(B\text{-}\alpha\text{-}SiW_9O_{34})][Ni_{0.5}(en)]\cdot 3.5H_2O$ (**8**),[14b] $[Ni(H_2O)_6][Ni_6(\mu_3\text{-}OH)_3(H_2O)_6(dap)_3(B\text{-}\alpha\text{-}SiW_9O_{34})]_2\cdot 8H_2O$ (**9**)[14a] and $[Ni(dap)_2][Ni_6(\mu_3\text{-}OH)_3(H_2O)_6(dap)_3(B\text{-}\alpha\text{-}SiW_9O_{34})]_2\cdot 10H_2O$ (**10**).[14a] Moreover, we also obtained an unprecedented double-cluster phosphotungstate simultaneously containing a hexa- and hepta-Ni^{II}-substituted trivacant Keggin clusters $[\{Ni_7(\mu_3\text{-}OH)_3O_2(dap)_3(H_2O)_6\}(B\text{-}\alpha\text{-}PW_9O_{34})][\{Ni_6(\mu_3\text{-}OH)_3(dap)_3(H_2O)_6\}(B\text{-}\alpha\text{-}PW_9O_{34})][Ni(dap)_2(H_2O)_2]\cdot 4.5H_2O$ (**11**).[14b] We extended the precursors from $[A\text{-}\alpha\text{-}PW_9O_{34}]^{9-}$ (A-α-

PW_9)[18a] or [A-α-SiW_9O_{34}]$^{10-}$ (A-α-SiW_9)[18b] to [A-α-GeW_9O_{34}]$^{10-}$ (A-α-GeW_9),[18c] and we isolated hexa-Ni^{II}-substituted trivacant Keggin germanotungstates **1** and **2**. However, the silicotungstates and germanotungstates similar to **4**–**7** and **11** were still not found hitherto in our search, and we presume that the possible reasons are related to the nature of the precursors. In addition, in the present research system, we can only introduce small organoamines [such as en, dap and diethylenetriamine (dien)] as SSAs to capture and stabilize the in situ formed hexa-Ni^{II} clusters. Nevertheless, the use of 1,3-diaminopropane or 1,6-diaminohexane in place of en or dap led to the formation of amorphous powders. However, when we employed larger organoamines [such as triethylenetetramine (teta) or tetraethylenepentamine (tepa)] as SSAs, hexa-Ni^{II}-substituted Keggin POMs were not formed, and we only obtained inorganic–organic hybrid tetra-Ni^{II}-sandwiched POT [Ni(tepa)$(H_2O)]_4H_2[Ni_4(H_2O)_2$(B-α-$PW_9O_{34})_2]\cdot 8H_2O$ (**12**).[14d] Therefore, the sizes and types of organoamines play an important role in the construction of hexa-Ni^{II} clusters under the studied system. In addition, under reaction conditions similar to those used for the preparation of **1**, **2** and **8**, when $NiCl_2\cdot 6H_2O$ was replaced by $CuCl_2\cdot 2H_2O$, we separated unprecedented inorganic–organic hybrid octa-Cu^{II}-sandwiched POTs $[Cu(H_2O)_2]H_2[Cu_8(dap)_4(H_2O)_2$(B-α-$GeW_9O_{34})_2]$ (**13**)[16] and $[Cu(dap)(H_2O)_3]_2[\{Cu_8(dap)_4$-$(H_2O)_2\}$(B-α-$SiW_9O_{34})_2]\cdot 6H_2O$ (**14**).[14b] Other TM ions, such as Co^{II}, Fe^{II}, Zn^{II}, Cd^{II}, Cr^{III} and Ti^{IV} ions, have also been investigated; however, no analogous silicotungstates and germanotungstates can be obtained. We also found that under reaction conditions similar to those used or the preparation of **1**, **2** and **8**, when [γ-$GeW_{10}O_{36}$]$^{8-}$ (γ-GeW_{10})[18d] or [γ-$SiW_{10}O_{36}$]$^{8-}$ (γ-SiW_{10})[18e] was replaced by A-α-GeW_9 or A-α-SiW_9, the hexa-Ni^{II}-substituted POTs can be also synthesized, which explains why γ-GeW_{10} and γ-SiW_{10} can easily isomerize into B-α-GeW_9 and B-α-SiW_9 under hydrothermal conditions. In addition, **1** and **2** may have undergone isomerization (A-α-GeW_9 → B-α-GeW_9), metal aggregation, or metal incorporation (Figure 1). Although the A-α-GeW_9 polyoxoanion was used as the starting material, both **1** and **2** contain the B-α-GeW_9 fragments, indicating that the isomerization of A-α-GeW_9 → B-α-GeW_9 must have taken place in the preparation of **1** and **2**. This isomerization occurs mostly because the A-α-GeW_9 unit has six exposed surface oxygen atoms in the vacant site, whereas the B-α-GeW_9 unit has seven exposed surface oxygen atoms, which allows the B-α-GeW_9 unit to act as a heptadentate ligand to coordinate to the hexa-Ni cluster that is formed in situ, thereby enhancing the chemical stability of **1** and **2**. On one hand, when the reaction is performed while heating, the isomerization of A-α-GeW_9 → B-α-GeW_9 is favoured,[6e,16] which is in good agreement with the driving force of isomerization controlled by the thermodynamic factors.[14a,14b] In 2004, Kortz et al. proved that the isomerization of A-α-GeW_9 → B-α-GeW_9 occurred during the course of the reaction of Cu^{II}, Mn^{II}, Zn^{II} and Cd^{II} ions with A-α-GeW_9 to prepare the sandwich-type species $[M_4(H_2O)_2$(B-α-$GeW_9O_{34})_2]^{12-}$ in an aqueous acidic medium upon heating. In the preparation of $[Cu(H_2O)_2]$-$H_2[Cu_8(dap)_4(H_2O)_2$(B-α-$GeW_9O_{34})_2]$ under hydrothermal conditions,[16] we also observed this transformation.

Table 1. Summary of synthetic conditions and related phases in the preparation of **1** and **2**.

Precursor	Precursor/M[a]/L[b]/H_2O (molar ratio)	Temperature / °C	Phase
A-α-GeW_9[c]	0.08:1.00:1.480:444	100	**1**
A-α-GeW_9	0.08:1.00:1.767:444	100	**2**
A-α-PW_9[d]	0.05:1.00:0.740:278	80	**3**[14b]
A-α-PW_9	0.05:1.00:0.740:278	130	**4**[14b]
A-α-PW_9	0.05:1.00:0.589:278	130	**5**[14b]
A-α-PW_9	0.12:3.37:3.534:554	170	**6**[14a]
A-α-PW_9	0.43:3.37:0.279:554	170	**7**[14a]
A-α-SiW_9[e]	0.08:1.00:1.480:444	80	**8**[14b]
A-α-SiW_9	0.10:3.37:3.534:554	170	**9**[14a]
A-α-SiW_9	0.26:0.84:1.178:554	170	**10**[14a]
A-α-PW_9	0.14:1.00:2.356:444	160	**11**[14b]
A-α-PW_9	0.09:0.500:0.264:278	160	**12**[14d]
A-α-GeW_9	0.08:0.75:0.589:278	100	**13**[16]
A-α-SiW_9	0.10:0.75:0.589:278	100	**14**[14b]

[a] M = Ni^{II} or Cu^{II}. [b] L represents en, dap, dien or tepa. [c] A-α-GeW_9: K_8Na_2[A-α-$GeW_9O_{34}]\cdot 25H_2O$.[18c] [d] A-α-PW_9: Na_9[A-α-$PW_9O_{34}]\cdot 7H_2O$.[18a] [e] A-α-SiW_9: K_{10}[A-α-$SiW_9O_{34}]\cdot 25H_2O$.[18b]

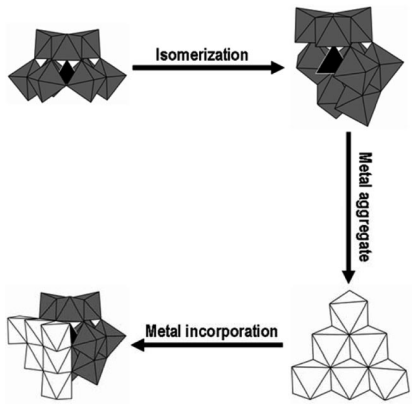

Figure 1. The schematic process of the isomerization of A-α-GeW_9 → B-α-GeW_9, aggregate of the hexa-Ni cluster and incorporation of the hexa-Ni cluster into the B-α-GeW_9 fragment.

IR Spectroscopy

The FTIR spectra of **1** and **2** display strong characteristic vibration bands in the 1000–400 cm^{-1} region, which is very similar to those of the trivacant polyoxoanion A-α-GeW_9, as a result of the fact that their polyoxoanions exhibit C_3 symmetry. In the low-wavenumber region (Figure 2), the IR spectra of **1** and **2** display characteristic vibration patterns derived from the trivacant Keggin-type precursor. Four characteristic vibration bands, namely, ν(W–O_t), ν(Ge–O_a), ν(W–O_b–W) and ν(W–O_c–W), appear at 938, 831, 770 and 700 cm^{-1} for **1** and at 936, 836, 769 and 691 cm^{-1} for **2**, respectively.[16] In general, these characteristic bands can be easily assigned by comparing the corresponding bands of the trivacant Keggin clusters. The stretching bands of the –OH, $–NH_2$ and $–CH_2$ groups are observed at, 3407, 3348–

3268 and 2936 cm^{-1} for **1** and at 3440, 3344–3282 and 2968 cm^{-1} for **2**, respectively. The bending vibration bands of the $–NH_2$ and $–CH_2$ groups appear at 1596 and 1459 cm^{-1} for **1** and at 1591 and 1458 cm^{-1} for **2**, respectively.[14b–14d,19] The occurrence of these vibration bands is indicative of the presence of organoamines in **1** and **2**, which is in good agreement with single-crystal structural analyses.

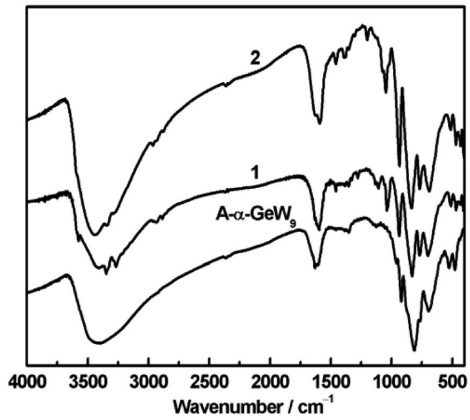

Figure 2. IR spectra of A-α-GeW_9O_{34}, **1** and **2**.

Structural Description

Compounds **1** and **2** are only synthesized under hydrothermal conditions and are inaccessible by the conventional aqueous solution method. Single-crystal X-ray diffraction analyses revealed that both **1** and **2** consist of two structural building units (SBUs), a B-α-GeW_9 fragment and a hexa-Ni^{II} cluster $\{Ni_6(\mu_3\text{-}OH)_3(L)_3(H_2O)_6\}$ (L = en for **1** and dap for **2**), which are combined together through one μ_4-O from the GeO_4 group and six μ_3-O from six WO_6 groups constructing the novel hexa-Ni^{II}-substituted trivacant Keggin POMs (Figure 3a,b). This structural type was first reported by us,[14a,14b] and these hexa-Ni^{II}-substituted POTs have become a family of novel and interesting TMSPs with ferromagnetic exchange interactions within magnetic centres in POM chemistry. As part of our continuous work, detailed comparisons of synthetic conditions (Table 1) and structural differences are provided in this paper. In a word, the successful preparations of these hexa-Ni^{II}-substituted POMs confirm that the combination of lacunary POM precursors and Ni^{II} complex cations under hydrothermal techniques is a very effective approach to make and construct TMSPs.

Compound **1** crystallizes in the monoclinic space group $P2_1/n$ and compound **2** belongs to the monoclinic space group $P2_1/c$ (Table 3). The molecular unit of **1** consists of a hexa-Ni^{II}-substituted SBU $[\{Ni_6(\mu_3\text{-}OH)_3(en)_3(H_2O)_6\}(B\text{-}\alpha\text{-}GeW_9O_{34})]^-$, half a $[Ni(en)_2]^{2+}$ complex cation as the charge balance ion and three lattice water molecules (Figure 3a), whereas the molecular unit of **2** comprises a hexa-Ni^{II}-substituted SBU $[\{Ni_6(\mu_3\text{-}OH)_3(dap)_3(H_2O)_6\}(B\text{-}\alpha\text{-}GeW_9O_{34})]^-$, one protonated water molecule as the charge balance ion and four lattice water molecules (Figure 3b). Notice that different cations in **1** and **2** lead to differences in their cell constants and crystallographic symmetry. Additionally, in order to determine the oxidation states of the W atoms in **2**, bond valence sum (BVS) calculations of W atoms were performed,[20] and the BVS values of the W1–

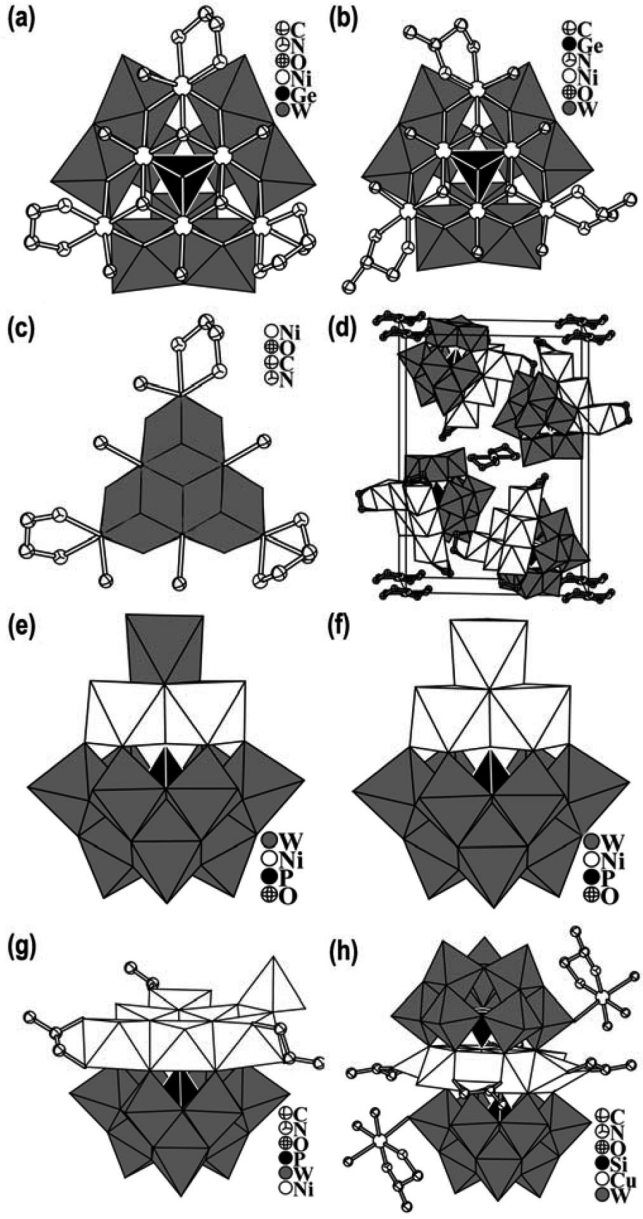

Figure 3. (a) Combined ball-and-stick/polyhedral representation of **1**; (b) combined ball-and-stick/polyhedral representation of **2**; (c) distribution motif of the $[Ni_6(\mu_3\text{-}OH)_3]^{9+}$ core as three edge-sharing truncated cubanes $Ni_3O_3(OH)$ in **1**; (d) view of the molecules of **1** in a unit cell; (e) polyhedral representation of $[Ni_3(H_2O)_3PW_{10}O_{39}H_2O]^{7-}$; (f) polyhedral representation of $[H_2PW_9Ni_4O_{34}(OH)_3(H_2O)_6]^{2-}$; (g) view of the hepta-Ni-substituted POM fragment in $[\{Ni_7(\mu_3\text{-}OH)_3O_2(dap)_3(H_2O)_6\}(B\text{-}\alpha\text{-}PW_9O_{34})][\{Ni_6(\mu_3\text{-}OH)_3(dap)_3(H_2O)_6\}(B\text{-}\alpha\text{-}PW_9O_{34})][Ni(dap)_2(H_2O)_2]\cdot 4.5H_2O$ (**11**); (h) view of the octa-Cu-sandwiched POM $[Cu(dap)(H_2O)_3]_2[\{Cu_8(dap)_4(H_2O)_2\}(B\text{-}\alpha\text{-}SiW_9O_{34})_2]\cdot 6H_2O$ (**14**). Discrete charge balance cations, hydrogen atoms and crystal water molecules were omitted for clarity.

W9 atoms are 6.30, 6.39, 6.37, 6.22, 6.18, 6.50, 6.36, 6.41 and 6.30, indicating the oxidation states of all the W atoms are +6. Therefore, the charge of the $[\{Ni_6(\mu_3\text{-}OH)_3(dap)_3(H_2O)_6\}(B\text{-}\alpha\text{-}GeW_9O_{34})]^-$ unit is –1. Considering the requirement of the charge balance of $[\{Ni_6(\mu_3\text{-}OH)_3(dap)_3(H_2O)_6\}(B\text{-}\alpha\text{-}GeW_9O_{34})]^-$, one H^+ ion is needed in the chemical formula of **2**, which is in accordance with the acidic environment of the reaction system of **2**. In fact, the phenomenon that the H^+ ions act as charge balance cations is very common in POM chemistry.[21] However, owing to the structural similarity of the hexa-Ni-substituted SBUs $[\{Ni_6(\mu_3\text{-}OH)_3(en)_3(H_2O)_6\}(B\text{-}\alpha\text{-}GeW_9O_{34})]^-$ for **1** and $[\{Ni_6(\mu_3\text{-}OH)_3(dap)_3(H_2O)_6\}(B\text{-}\alpha\text{-}GeW_9O_{34})]^-$ for **2**, only the structure of **1** is described in detail. In **1** and **2**, the B-α-GeW_9 SBU is the well-known trivacant Keggin fragment obtained by removing three edge-sharing WO_6 octahedra from the saturated $[\alpha\text{-}GeW_{12}O_{40}]^{4-}$ polyoxoanion, whereas another SBU, the Ni_6-containing $\{Ni_6(\mu_3\text{-}OH)_3(L)_3(H_2O)_6\}$ cluster, was already observed by us in hexa-Ni^{II}-substituted phosphotungstates and silicotungstates.[14a,14b] In **1**, the $\{Ni_6(\mu_3\text{-}OH)_3(en)_3(H_2O)_6\}$ cluster contains a hexanuclear $[Ni_6(\mu_3\text{-}OH)_3]^{9+}$ core (Figure 4a), induced by the trivacant sites of the B-α-GeW_9 unit, which is built by six nearly coplanar Ni^{II} ions with a triangle motif linked together by three μ_3-OH bridges [Ni–μ_3-O_{OH} 2.023(11)–2.056(11) Å], stabilized by six μ_3-O bridges from the lacunae of the B-α-GeW_9 moiety [Ni–μ_3-O 2.057(10)–2.180(12) Å] and one μ_4-O bridge from the central GeO_4 unit [Ni–μ_4-O 2.057(10)–2.096(11) Å]. Subsequently, the octahedral coordination sphere of each Ni ion is completed by en or water ligands [Ni–N 2.036(15)–2.104(16) Å and Ni–O_W 2.053(11)–2.166(13) Å]. Furthermore, in the $[Ni_6(\mu_3\text{-}OH)_3]^{9+}$ core, each one of three interior Ni (Ni4–Ni6) atoms is located at the trivacant sites of the B-α-GeW_9 unit and bonds to one water molecule, whereas each one of the three exterior Ni (Ni1–Ni3) atoms coordinates to one bidentate en and one water molecule, respectively, resulting in the formation of the $\{Ni_6(\mu_3\text{-}OH)_3(en)_3(H_2O)_6\}$ cluster. The $\{Ni_6(\mu_3\text{-}OH)_3(en)_3(H_2O)_6\}$ cluster caps the B-α-GeW_9 unit through the exposed seven bridging O atoms from the lacunae of the B-α-GeW_9 unit, that is, one μ_4-O from one GeO_4 group and six μ_3-O from six WO_6 groups, forming a new hexa-Ni^{II}-substituted POT **1**. Three μ_3-OH bridges and six terminal water molecules are determined by the BVS calculations.[20] In addition, the distribution motif of the six octahedral coordinate Ni^{II} ions exhibits a completely triangular arrangement, and the three exterior Ni (Ni_{ex}) atoms are situated in the three corners of the triangle with $Ni_{ex}\cdots Ni_{ex}$ distances of 6.185(3)–6.203(3) Å, whereas the three interior Ni (Ni_{in}) atoms are positioned at the midpoints of three edges with $Ni_{in}\cdots Ni_{in}$ or $Ni_{ex}\cdots Ni_{in}$ separations of 3.079(3)–3.122(3) Å. Alternatively, the distribution motif of the $[Ni_6(\mu_3\text{-}OH)_3]^{9+}$

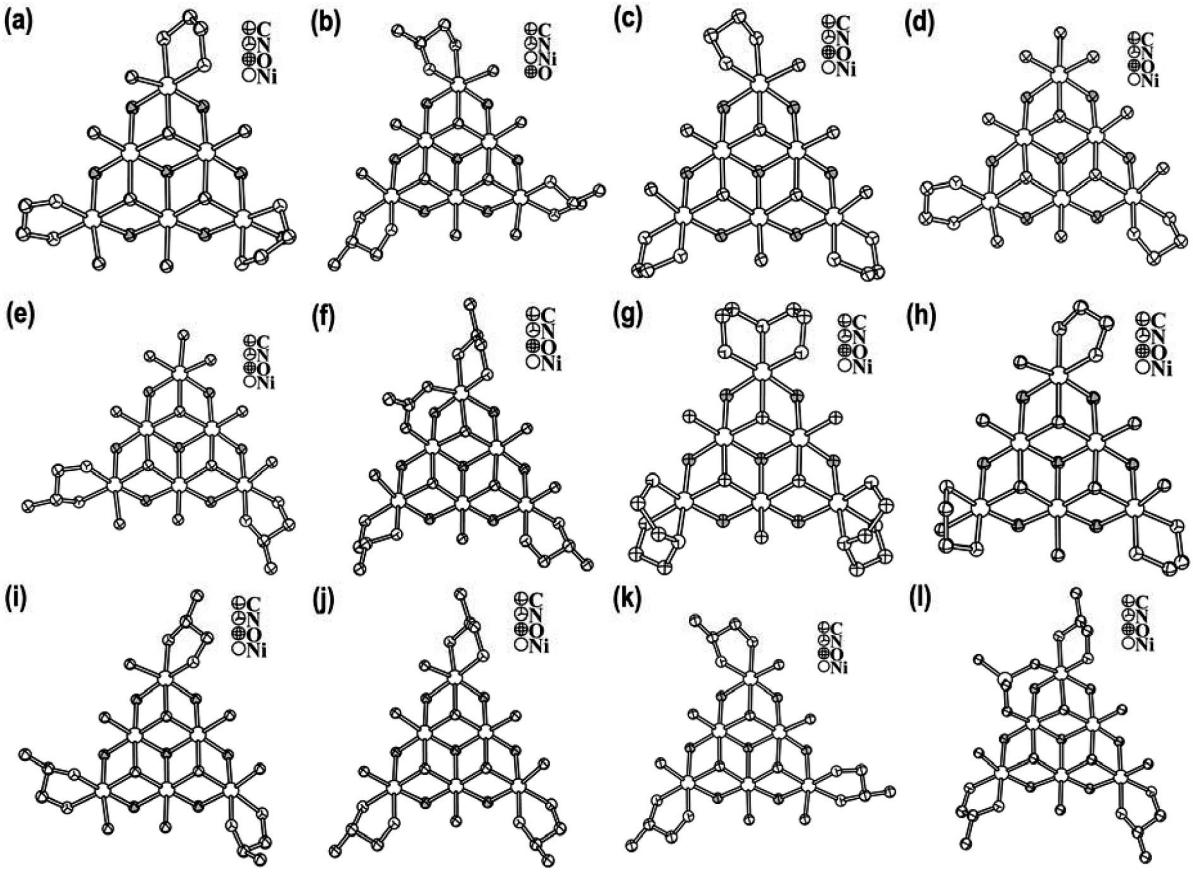

Figure 4. Ball-and-stick illustrations of the hexa-Ni^{II} units in **1** (a), **2** (b), **3** (c), **4** (d), **5** (e), **6** (f), **7** (g), **8** (h), **9** (i), **10** (j), **11** (k) and the hepta-Ni^{II} unit in **11** (k). Grey oxygen atoms are from B-α-XW_9 fragments.

core is also visualized as three edge-sharing truncated cubanes, $Ni_3O_3(OH)$ (Figure 3c). Interestingly, the hexa-Ni^{II}-substituted polyoxoanions $[\{Ni_6(\mu_3\text{-}OH)_3(en)_3(H_2O)_6\}(B\text{-}\alpha\text{-}GeW_9O_{34})]^-$ of **1** are distributed in four distinct orientations in a unit cell, whereas the discrete charge balance cations $[Ni(en)_2]^{2+}$ are situated on eight vertices and the body-centre of the unit cell (Figure 3d). Additionally, the water and diamine ligands on the hexa-Ni^{II} clusters $\{Ni_6(\mu_3\text{-}OH)_3(L)_3(H_2O)_6\}$ are good electron donors for the derivation of the supramolecular structures through hydrogen bonds (Table 2).

By close inspection of the hexa-Ni^{II} clusters $\{Ni_6(\mu_3\text{-}OH)_3(L)_3(H_2O)_6\}$ in **1**, **2** and **3**–**11**,[14a,14b] the coordination water molecules and organoamine ligands on the hexa-Ni^{II} units have different coordination orientations (Figure 4a–k). Moreover, these water ligands provide the likelihood that they may further be substituted by other ligands to generate unprecedented or extended structures. On one hand, the water ligands can be substituted by some small inorganic or organic groups to produce new discrete structures. For instance, the hexa-Ni^{II} $\{Ni_6(\mu_3\text{-}OH)_3(dap)_3(CH_3COO)(H_2O)_4\}$ (Figure 4f) cluster in **6** can be viewed as the product of a CH_3COO^- substitution for two neighbouring water ligands on the $\{Ni_6(\mu_3\text{-}OH)_3(dap)_3(H_2O)_6\}$ (Figure 4j) cluster.[14a] The hepta-Ni^{II} $[\{Ni_7(\mu_3\text{-}OH)_3O_2(dap)_3(H_2O)_6\}(B\text{-}\alpha\text{-}PW_9O_{34})]^{2-}$ (Figure 4l) cluster in **11** can be considered to be formed by two oxygen atoms of the $Ni_7O_2(H_2O)_2$ tetrahedron by replacing adjacent terminal water ligands on the $\{Ni_6(\mu_3\text{-}OH)_3(dap)_3(H_2O)_6\}$ cluster (Figure 4j).[14b] On the other hand, the water ligands can be substituted by the terminal oxygen atoms from POM units to construct novel multidimensional architectures. For example, one water ligand on the $\{Ni_6(\mu_3\text{-}OH)_3(dien)_3(H_2O)_3\}$ cluster is substituted by a terminal oxygen atom from an adjacent B-α-PW_9 unit, forming 1D zigzag chain **7**.[14a] A 3D hexa-Cu-substituted POT $[Cu_6(\mu_3\text{-}OH)_3(en)_3(H_2O)_3(B\text{-}\alpha\text{-}PW_9O_{34})]\cdot 7H_2O$ with 4^96^6 topology can be viewed to be formed by three terminal oxygen atoms from three adjacent B-α-PW_9 units by substituting the three terminal water ligands on the $\{Cu_6(\mu_3\text{-}OH)_3(en)_3(H_2O)_6\}$ unit.[14b] In short, the successful preparations of **6**, **7**, **11** and $[Cu_6(\mu_3\text{-}OH)_3(en)_3(H_2O)_3(B\text{-}\alpha\text{-}PW_9O_{34})]\cdot 7H_2O$ further consolidate the concept that the water ligands on the $\{Ni_6(\mu_3\text{-}OH)_3(L)_3(H_2O)_6\}$ or $\{Cu_6(\mu_3\text{-}OH)_3(L)_3(H_2O)_6\}$ clusters are the active sites for deriving novel high-nuclear TMSPs.

Although two tri-/tetra-Ni^{II}-substituted phosphotungstates $[Ni_3(H_2O)_3PW_{10}O_{39}H_2O]^{7-}$[3f] (Figure 3e) and $[H_2PW_9Ni_4O_{34}(OH)_3(H_2O)_6]^{2-}$[11] (Figure 3f) based on a single trivacant Keggin fragment capped by a cubane-like unit have been reported, to the best of our knowledge, hexa-Ni^{II}-substituted trivacant Keggin POTs obtained by us represent the first type of TMSPs anchoring the maximum 3d TM centres in a single trivacant Keggin or Dawson POM fragment to date, except for only one hepta-Ni^{II}-substituted fragment $[\{Ni_7(\mu_3\text{-}OH)_3O_2(dap)_3(H_2O)_6\}(B\text{-}\alpha\text{-}PW_9O_{34})]$ (Figure 3g and Figure 4l) in a novel double-cluster phosphotungstate $[\{Ni_7(\mu_3\text{-}OH)_3O_2(dap)_3(H_2O)_6\}(B\text{-}\alpha\text{-}PW_9O_{34})][\{Ni_6(\mu_3\text{-}OH)_3(dap)_3(H_2O)_6\}(B\text{-}\alpha\text{-}PW_9O_{34})][Ni(dap)_2(H_2O)_2]\cdot 4.5H_2O$ addressed by us recently.[14b] As far as we know, a hexa-Ni^{II}-sandwiched POT $K_6Na_4[\{Ni_6(H_2O)_4(\mu_2\text{-}H_2O)_4(\mu_3\text{-}OH)_2\}(SiW_9O_{34})_2]\cdot 17.5H_2O$,[3h] and three hexa-$Cu^{II}$-substituted POTs $(n\text{BuNH}_3)_{12}[(CuCl)_6(AsW_9O_{33})_2]\cdot 6H_2O$,[6f] $[Cu_6(\mu_3\text{-}OH)_3(en)_3(H_2O)_3(B\text{-}\alpha\text{-}PW_9O_{34})]\cdot 7H_2O$[14b] and $[Cu(dap)_2]_2\{[Cu(dap)_2(H_2O)]_2[Cu_6(dap)_2(B\text{-}\alpha\text{-}SiW_9O_{34})_2]\}\cdot 4H_2O$[15] have been reported. In $K_6Na_4[\{Ni_6(H_2O)_4(\mu_2\text{-}H_2O)_4(\mu_3\text{-}OH)_2\}(SiW_9O_{34})_2]\cdot 17.5H_2O$, the hexa-$Ni^{II}$ cluster is built by two Ni_3O_{13} seg-

Table 2. Hydrogen-bonding interactions in **1** and **2**.

D–H···A	*d*(D···A)	<(DHA)
1		
O(36)–H(36A)···O(13)#2[a]	2.879(16)	167.7
O(37)–H(37A)···O(12)#2[a]	2.983(17)	131.5
N(1)–H(1C)···O(25)	3.25(2)	136.1
N(1)–H(1C)···O(26)	3.08(2)	115.3
N(2)–H(2C)···O(29)#2[a]	2.914(19)	144.6
N(2)–H(2D)···O(20)#3[a]	2.972(19)	148.4
N(2)–H(2D)···O(4W)	3.152(18)	123.2
N(5)–H(5C)···O(23)#3[a]	3.01(2)	170.8
N(5)–H(5D)···O(32)#2[a]	3.154(18)	167.9
N(6)–H(6C)···O(6W)	3.11(2)	151.1
N(6)–H(6D)···O(28)#4[a]	2.940(18)	142.5
N(3)–H(3C)···O(29)	3.152(19)	135.6
N(3)–H(3C)···O(31)	3.169(19)	128.7
N(3)–H(3D)···O(1)#5[a]	3.182(19)	142.8
N(3)–H(3D)···O(3)#5[a]	3.231(18)	126.2
N(4)–H(4C)···O(7W)	3.06(3)	152.2
N(4)–H(4D)···O(5W)	3.17(2)	149.1
N(7)–H(7C)···O(6)#1[a]	3.13(2)	141.1
N(7)–H(7C)···O(7)#1[a]	3.322(19)	135.3
N(7)–H(7D)···O(8W)	3.01(3)	155.4
N(7)–H(7D)···O(1)#1[a]	3.13(2)	117.9
N(8)–H(8C)···O(8W)	3.01(3)	154.6
N(8)–H(8D)···O(25)#1[a]	3.13(2)	136.8
N(8)–H(8D)···O(6)#1[a]	3.20(2)	137.8
N(8)–H(8D)···O(10)#1[a]	3.25(2)	139.1
2		
O(35)–H(35A)···O(3)#2[b]	2.99(2)	170.2
O(36)–H(36A)···O(5)#2[b]	3.50(2)	162.6
O(37)–H(37A)···O(14)#2[b]	3.08(2)	156.5
N(1)–H(1C)···O(9W)	2.97(4)	135.2
N(1)–H(1C)···O(26)	3.17(3)	132.9
N(1)–H(1D)···O(29)	3.05(3)	154.5
N(2)–H(2B)···O(5W)	3.06(3)	151.4
N(2)–H(2C)···O(23)#2[b]	2.70(3)	116.2
N(3)–H(3D)···O(6W)	3.13(3)	148.8
N(4)–H(4C)···O(29)#3[b]	3.23(3)	142.9
N(4)–H(4D)···O(16)	3.11(3)	144.4
N(4)–H(4D)···O(17)	3.26(3)	124.5
N(5)–H(5B)···O(7)#4[b]	3.18(3)	151.1
N(5)–H(5B)···O(10)#4[b]	3.11(2)	126.6
N(5)–H(5C)···O(22)	3.14(3)	131.1
N(5)–H(5C)···O(23)	3.11(3)	123.5
N(6)–H(6D)···O(4W)	3.17(3)	120.3
N(6)–H(6E)···O(10W)#2[b]	3.15(5)	130.2
N(6)–H(6E)···O(1)#2[b]	3.32(3)	133.7

[a] Symmetry transformations used to generate equivalent atoms: #1: $-x + 2, -y, -z$; #2: $x + 1/2, -y + 1/2, z + 1/2$; #3: $-x + 2, -y, -z + 1$; #4: $x - 1/2, -y + 1/2, z + 1/2$; #5: $-x + 3/2, y + 1/2, -z + 1/2$. [b] Symmetry transformations used to generate equivalent atoms: #1: $-x + 1, -y, -z + 1$; #2: $x, -y + 1/2, z - 1/2$; #3: $-x, -y, -z$; #4: $-x, y + 1/2, -z + 1/2$.

ments linked through two μ_3-OH groups.[3h] In $(n\text{BuNH}_3)_{12}$-$[(\text{CuCl})_6(\text{AsW}_9\text{O}_{33})_2]\cdot 6\text{H}_2\text{O}$, the hexa-$\text{Cu}^{\text{II}}$ cluster is a hexagonal alignment made up of six edge-sharing CuO_4Cl square pyramids.[6f] In $[\text{Cu}_6(\mu_3\text{-OH})_3(\text{en})_3(\text{H}_2\text{O})_3$-$(\text{B-}\alpha\text{-PW}_9\text{O}_{34})]\cdot 7\text{H}_2\text{O}$, the structure of the hexa-Cu^{II} cluster is similar to those in **1** and **2**, and the distribution motif of six edge-sharing octahedral Cu^{II} ions also shows a triangular arrangement.[14b] In $[\text{Cu(dap)}_2]_2\{[\text{Cu(dap)}_2(\text{H}_2\text{O})]_2[\text{Cu}_6$-$(\text{dap})_2(\text{B-}\alpha\text{-SiW}_9\text{O}_{34})_2]\}\cdot 4\text{H}_2\text{O}$, the hexa-$\text{Cu}^{\text{II}}$ cluster exhibits a belt-like structure with an edge-sharing combination of CuO_6 octahedra and CuO_5 and CuO_3N_2 square pyramids.[15] In addition, in our exploration, two novel inorganic–organic hybrid octa-Cu^{II}-sandwiched POTs $[\text{Cu}$-$(\text{dap})(\text{H}_2\text{O})_3]_2[\{\text{Cu}_8(\text{dap})_4(\text{H}_2\text{O})_2\}(\text{B-}\alpha\text{-SiW}_9\text{O}_{34})_2]\cdot 6\text{H}_2\text{O}$ (**14**)[14b] (Figure 3g) and $[\text{Cu(H}_2\text{O})_2]\text{H}_2[\text{Cu}_8(\text{dap})_4(\text{H}_2\text{O})_2(\text{B-}$ $\alpha\text{-GeW}_9\text{O}_{34})_2]$ (**13**)[16] were found, where the distribution of eight Cu^{II} ions in the sandwich belt illustrates the 3:2:3 motif.

Magnetic Properties

The ability of lacunary polyoxoanions to incorporate magnetic TM clusters between nonmagnetic POM fragments makes them especially valuable for the quantification of magnetic interactions;[22] therefore, it is necessary that we quantitatively describe the magnetic exchange interactions within the hexa-Ni^{II} clusters in **1** and **2**. Owing to the structural similarity of the hexa-Ni^{II} clusters in **1** and **2**, the experimental magnetic susceptibilities were fitted to a theoretical model (Figure 5a). The molar magnetic susceptibility (χ_M) and its temperature product ($\chi_M T$) versus T plots for **1** and **2** under an external magnetic field of 5 kOe are shown in Figure 5a and b, respectively. The value of χ_M for **1** (or **2**) gradually increases from 0.026 (0.025) emu mol^{-1} at 300 K to 0.303 (0.302) emu mol^{-1} at 49 K, then sharply to the maximum value of 7.600 (7.105) emu mol^{-1} at 2 K. The value of $\chi_M T$ for **1** (or **2**) increases upon cooling from 7.845 (7.808) emu mol^{-1} K at 300 K, which is slightly higher than the sum of the spin-only contributions (7.512 emu mol^{-1} K for 6.5 noncorrelated Ni^{II} ions for **1** and 6.934 emu mol^{-1} K for 6 noncorrelated Ni^{II} ions for **2**) with g = 2.15, and it reaches a maximum of 22.100 (21.926) emu mol^{-1} K at 11 (12) K. This behaviour of the $\chi_M T$ versus T plots for **1** and **2** shows the presence of overall ferromagnetic coupling interactions with S = 6 spin ground state for the hexa-Ni^{II} cluster in **1** and **2**.[3f,8,14] This observation is in accordance with the dependence of magnetization on the magnetic field performed at T = 2 K (see below). A sudden decrease in the $\chi_M T$ value below 11 K for **1** (12 K for **2**) suggests the presence of the significant zero-field splitting (ZFS) effects in the ground state or molecular interactions. It is worth noting that in previous work investigators showed that the behaviour of $\chi_M T$ at very low temperatures may be related to an anisotropic coupling of the Ni^{II} ions inside the cluster rather than to a mean-field correction.[3f,5] The best fit of the Curie–Weiss law on the correlation between the inverse magnetic susceptibility χ_M^{-1} and temperature T in the range 50–300 K yields the Curie constant C = 7.091 emu K mol^{-1} and Weiss constant θ = 31.301 K for **1** (C = 7.074 emu K mol^{-1} and θ = 31.635 K for **2**; Figure 6), which further support overall ferromagnetic exchange interactions. As the temperature decreases from 50 to 2 K, the Curie–Weiss law is not followed, possibly resulting from the presence of the significant ZFS effect. The field (H) dependency of the magnetization (M) in electron Bohr magneton (μ_B) per mol units for **1** and **2** at 2 K are shown in Figure 7. The magnetization of **1** and **2** increases with increasing field with an approximately linear relationship at $H < 10$ kOe and then reaches the values of 13.0 and 12.5 μ_B for **1** and **2** at 70 kOe, respectively, which are close to the saturation values expected for a hexa-Ni^{II} cluster (S = 6) and half Ni^{II} ion (S = 1) for **1** and a hexa-Ni^{II} cluster (S = 6) for **2** with ferromagnetic interactions.

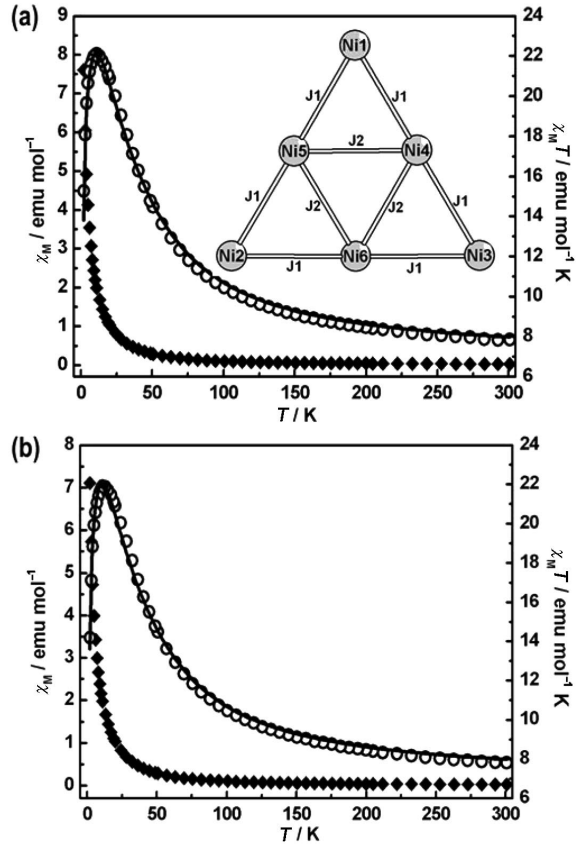

Figure 5. Plots of χ_M and $\chi_M T$ vs. T in the temperature range 2–300 K for **1** (a) and **2** (b) under an applied magnetic field of 5 kOe. Solid lines represent the best fitting to the experimental data. The inset is a magnetic exchange model used for the hexa-Ni^{II} clusters in **1** and **2**.

For quantitative analyses of the magnetic exchange interactions, the magnetic properties of **1** and **2** were theoretically analyzed by the isotropic Heisenberg exchange Hamiltonian by taking into account the ZFS effects regardless of the second- and third-neighbour interactions between the Ni^{II} ions with significantly long distances (more than

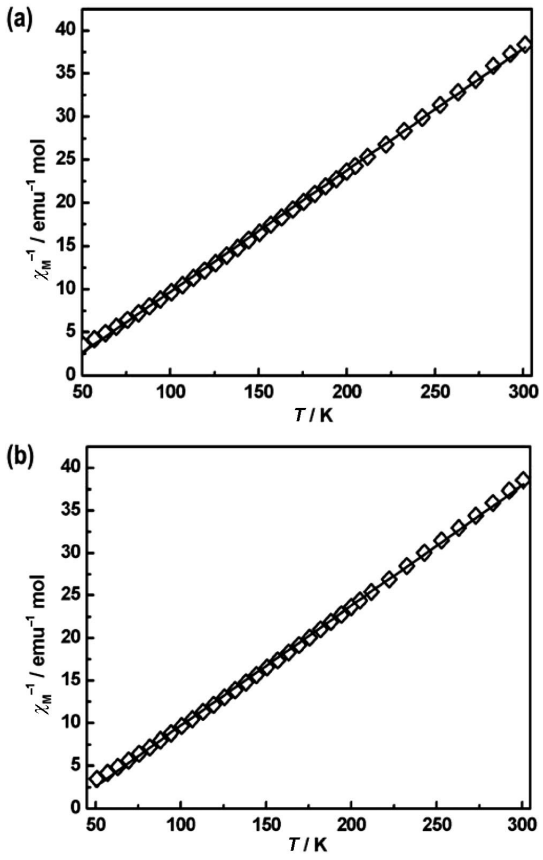

Figure 6. Temperature dependence of the inverse magnetic susceptibilities (χ_m^{-1}) for **1** (a) and **2** (b) between 50 and 300 K. Solid lines are generated from the best fit by the Curie–Weiss expression.

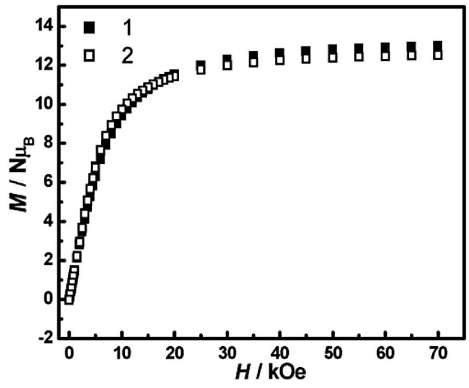

Figure 7. Magnetization as a function of the applied field recorded at 2 K.

5.4 Å). The appropriate Hamiltonian for hexa-Ni^{II} clusters in **1** and **2** by using the isotropic model can be written as Equation (1) with $S_1 = S_2 = S_3 = S_4 = S_5 = S_6 = 1$.

$$H = -2J_1(S_1S_4 + S_1S_5 + S_2S_5 + S_2S_6 + S_3S_4 + S_3S_6) - 2J_2(S_4S_5 + S_4S_6 + S_5S_6) + \Sigma DS_{iZ}^2 \quad (1)$$

where J_1 is the exchange constant between the Ni^{II} ions situated in the corners of an equilateral triangle and the Ni^{II} ions sitting on the edge midpoint of an equilateral triangle; J_2 is the exchange constant between the Ni^{II} ions sitting on the edge midpoint of an equilateral triangle (Figure 5a) and D represents the ZFS parameter. Note that the discrete $[Ni(en)_2]^{2+}$ ion in **1** is treated as a paramagnetic ion. Calculations were performed by using the MAGPACK package.[23]

Excellent agreement with the experimental data was obtained with the following set of parameters: $J_1 = 0.68$ cm^{-1}, $J_2 = 1.48$ cm^{-1}, $g = 2.14$, $D = 1.39$ cm^{-1} and the agreement factor $R = 3.63 \times 10^{-4}$ for **1**, and $J_1 = 0.67$ cm^{-1}, $J_2 = 1.52$ cm^{-1}, $g = 2.14$, $D = 1.48$ cm^{-1} and the agreement factor $R = 2.86 \times 10^{-4}$ for **2**, which confirm ferromagnetic coupling interactions among the Ni^{II} centres. Moreover, these data are in good agreement with those of the hexa-Ni^{II}-substituted phosphotungstate $[\{Ni_6(\mu_3\text{-}OH)_3(en)_3(H_2O)_6\}(B\text{-}\alpha\text{-}PW_9O_{34})]\cdot 7H_2O$ reported by us.[14b] In addition, to determine the magnitude of the rhombic magnetic anisotropy parameter E and to characterize the ground state of **1**, magnetization data were collected in the 1–6 T (1 T = 10000 Oe) field range and 2–6 K temperature range to complement the available 0.5 T data. Shown in Figure 8 is a plot of the data as reduced magnetization (M / Nμ_B) versus H/T, where N is Avogadro's number and μ_B is the Bohr magneton. For a system occupying only the ground state and experiencing no ZFS effects, the various isofield lines would be superimposed and M would saturate at a value of gS. The non-superimposition of the isofield lines clearly indicates the presence of ZFS effects.[24a,24b] The postulated spin Hamiltonian can be expressed in its simplest form by [Equation (2)].[24c]

$$H = g\mu_B HS + D[S_z^2 - (1/3)S(S+1)] + E(S_x^2 - S_y^2) \quad (2)$$

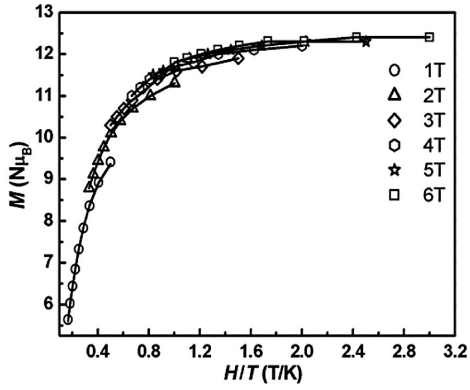

Figure 8. Plots of reduced magnetization vs. H/T for **1** at the indicated applied fields. The isofield lines are least-square fits to the data according to Equation 2.

The solid lines in Figure 8 represent the least-square fits of the six isofield magnetization data sets recorded for **1**. The best fitting leads to the rhombic magnetic anisotropy parameter $E = 4.14 \times 10^{-5}$. Thus, E is so small that it can be neglected. Omission of the E parameter is commonly encountered in Ni-substituted POMs.[3f] For example, the magnetic fitting of $[Ni_3(H_2O)_3(PW_{10}O_{39})H_2O]^{7-}$ and $[Ni_4(H_2O)_2(PW_9O_{34})_2]^{10-}$ only gave their D parameters of 5.8 and 4.5 cm^{-1}, respectively.[3f] According to the previous

study,[3f,5,25] the magnetic interactions are highly sensitive to the values of the Ni–O–Ni bridging angles: the interactions are ferromagnetic for angles in the range of 90 ± 14°, whereas they are antiferromagnetic for larger angles. A comparison of the structural parameters obtained in the present study shows that such an explanation is satisfying: the Ni–O–Ni angles vary between 93.2(4) and 100.4(5)° for **1** and between 94.1(6) and 100.3(6)° for **2**; therefore, dominant ferromagnetic exchange interactions are not unexpected for **1** and **2**. Besides ferromagnetic couplings in the coplanar hexa-Ni^{II} clusters, ferromagnetic exchange interactions in the coplanar tetra-Ni^{II} clusters have been reported in sandwich-type TMSPs.[3f,14c,14d] Moreover, the ferromagnetic coupling in the cubane Ni_4O_4 cluster unit in $Cs_2[H_2PW_9Ni_4O_{34}(OH)_3(H_2O)_6]\cdot 5H_2O$ was investigated by Kortz et al.[11] In addition, the tri-Ni^{II} clusters incorporated in lacunary POM fragments, such as $[Ni_3Na(H_2O)_2(AsW_9O_{34})_2]^{11-}$[5] and $[Ni_3(H_2O)_3(PW_{10}O_{39})H_2O]^{7-}$,[3f] also indicate the occurrence of ferromagnetic exchange interactions.

Thermogravimetric Analyses

The thermogravimetric behaviour of compounds **1** and **2** was investigated (Figure 9), and the weight-loss processes of **1** and **2** can be divided into three steps in the range of 30–800 °C. For **1**, the first weight loss of 1.45% between 30 and 144 °C is assigned to the release of three lattice water molecules (calcd. 1.74%). The second weight loss of 3.82% between 144 and 330 °C is ascribed to the loss of six coordinated water ligands (calcd. 3.48%). The third weigh loss of 8.72% from 330 to 800 °C corresponds to the removal of four en ligands and the dehydration of three hydroxy groups. For **2**, owing to the first two weight-loss steps with amphibolous limits, the combined weight loss of the first and second steps is 6.89% between 30 and 323 °C, assigned to the removal of five lattice water molecules and six coordinated water ligands (calcd. 6.49%). The third weight loss is 8.88% from 323 to 800 °C and corresponds to the release of three dap ligands and the dehydration of three hydroxy groups and one proton (calcd. 8.41%). The above-mentioned analyses reveal that the experimental values are consistent with the theoretical values.

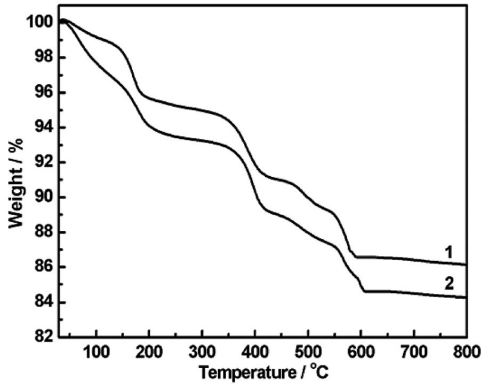

Figure 9. The thermogravimetric curves of **1** and **2** measured in the range 30–800 °C under a dry air atmosphere with a heating rate of 10 °C min^{-1}.

Conclusions

The successful preparations of two new inorganic–organic hybrid hexa-Ni^{II}-cluster-substituted germanotungstates $[Ni(en)_2]_{0.5}[\{Ni_6(\mu_3\text{-}OH)_3(en)_3(H_2O)_6\}(B\text{-}\alpha\text{-}GeW_9O_{34})]\cdot 3H_2O$ (**1**) and $[Ni_6(\mu_3\text{-}OH)_3(dap)_3(H_2O)_6][B\text{-}\alpha\text{-}GeW_9O_{34}]\cdot H_3O\cdot 4H_2O$ (**2**) further prove that it is effective for the synthetic strategy of using the lacunary sites of the α-XW_9O_{34} (X = P, Si, Ge) fragment as structure-directing agents to induce the formation of large oligomers of TM clusters and the multidentate amines as structure-stabilizing agents to capture and stabilize the in situ formed large oligomers of TM clusters to construct novel TMSP materials under hydrothermal conditions.[14] Furthermore, the magnetic properties of **1** and **2** were quantitatively analyzed by an isotropic Heisenberg exchange model by taking into account the ZFS effects. Like the Cu_6 and Mn_6 hexagonal clusters reported by Yamase et al.,[6f] the in situ formed hexa-Ni^{II} clusters in **1** and **2** induced by the α-GeW_9O_{34} fragment are not only a simple model for exchange–interaction study of molecular magnets but also provide a molecular design for novel magnetic devices.

Experimental Section

General: The precursor $K_8Na_2[A\text{-}\alpha\text{-}GeW_9O_{34}]\cdot 25H_2O$[18c] was synthesized as described in the literature and its purity was verified by IR spectroscopy. Other chemical reagents were used as commercially purchased without further purification. C, H and N elemental analyses were determined with a Vario EL III elemental analyzer. Infrared spectra for solid samples were obtained as KBr pellets with an ABB Bomen MB 102 FTIR spectrometer in the range 4000–400 cm^{-1}. Magnetic susceptibility measurements were carried out with a Quantum Design MPMS-5 magnetometer in the temperature range 2–300 K. The susceptibility data were corrected from the diamagnetic contributions as deduced by using Pascal's constant tables. Thermogravimetric analyses were performed with a Mettler TGA/SDTA851 thermal analyzer in a flowing air atmosphere with a heating rate of 10 °C min^{-1} in the temperature region 30–1000 °C.

$[Ni(en)_2]_{0.5}[\{Ni_6(\mu_3\text{-}OH)_3(en)_3(H_2O)_6\}(B\text{-}\alpha\text{-}GeW_9O_{34})]\cdot 3H_2O$ (1): $K_8Na_2[A\text{-}\alpha\text{-}GeW_9O_{34}]\cdot 25H_2O$ (0.246 g, 0.080 mmol), $NiCl_2\cdot 6H_2O$ (0.237 g, 1.000 mmol), en (0.10 mL, 1.480 mmol) were successively suspended in H_2O (8 mL, 444 mmol), and the mixture was stirred for 1.5 h, sealed in a 20-mL Teflon-lined steel autoclave, kept at 100 °C for 5 d and then cooled to room temperature. Green prismatic crystals were obtained by filtering, washed with distilled water and dried in air. The crystals were collected mechanically. Yield: ca. 35% (based on $K_8Na_2[A\text{-}\alpha\text{-}GeW_9O_{34}]\cdot 25H_2O$). $C_8H_{53}GeN_8Ni_{6.5}O_{46}W_9$ (3106.44): calcd. C 3.09, H 1.72, N 3.61; found C 2.98, H 1.65, N 3.36.

$[\{Ni_6(dap)_3(H_2O)_6(OH)_3\}(B\text{-}\alpha\text{-}GeW_9O_{34})]\cdot H_3O\cdot 4H_2O$ (2): The synthetic method is identical to that of **1** with dap (0.15 mL, 1.767 mmol) in place of en. Yield: ca. 43% (based on $K_8Na_2[A\text{-}\alpha$-

$GeW_9O_{34}]\cdot 25H_2O$). $C_9H_{54}GeN_6Ni_6O_{47}W_9$ (3077.89): calcd. C 3.51, H 1.77, N 2.73; found C 3.68, H 2.03, N 2.89.

X-ray Structure Determination: A suitable single crystal of the as-synthesized compound with dimensions of $0.15\times0.07\times0.04$ mm for **1** and $0.25\times0.15\times015$ nm for **2** was carefully selected under an optical microscope and glued to a thin glass fibre with epoxy resin. Crystal structure determinations by X-ray diffraction were performed with a Siemens SMART CCD diffractometer for **1** and RIGAKU Mercury 70 CCD diffractometer for **2** with graphite-monochromated Mo-K_α (λ = 0.71073 Å) radiation at room temperature. The structures were solved by direct methods. The tungsten, nickel and germanium atoms were first located, and the carbon, nitrogen and oxygen atoms were found in the successive difference Fourier maps by using the SHELX97 program package.[26] The structures were refined on F^2 by full-matrix least-squares methods. An empirical absorption correction was applied. No hydrogen atoms associated with water molecules were located from the difference Fourier maps. Hydrogen atoms attached to carbon and nitrogen atoms were geometrically placed. All hydrogen atoms were refined isotropically as a riding mode by using the default SHELXTL parameters. All non-hydrogen atoms were refined anisotropically. The crystallographic data for **1** and **2** are presented in Table 3. CCDC-669946 (for **1**) and -669947 (for **2**) contain the crystallographic data for this paper. These data can be obtained free of charge from The Cambridge Crystallographic Data Centre via www.ccdc.cam.ac.uk/data_request/cif.

Table 3. Crystallographic data and structure refinements of **1** and **2**.

	1	**2**
Empirical formula	$C_8H_{53}N_8O_{46}Ni_{6.5}GeW_9$	$C_9H_{54}N_6O_{47}Ni_6GeW_9$
Fw	3106.44	3077.89
Crystal system	monoclinic	monoclinic
Space group	$P2_1/n$	$P2_1/c$
a / Å	12.9432(3)	13.919(16)
b / Å	23.5840(5)	23.73(3)
c / Å	17.0394(4)	18.815(16)
β / °	102.17	115.77(6)
Volume / Å^3	5084.4(2)	5596(11)
Z	4	4
$d_{calcd.}$ / g cm^{-3}	4.058	3.653
Crystal size / mm	$0.15\times0.07\times0.04$	$0.16\times0.10\times0.05$
Index range	$-15\le h\le 15$	$-16\le h\le 13$
	$-28\le k\le 15$	$-27\le k\le 28$
	$-18\le l\le 20$	$-22\le l\le 22$
Measured reflns.	23801	32634
Unique reflns.	8862	9707
R_{int}	0.0986	0.0685
Wavelength / Å	0.71073	0.71073
Abs. coeff. / mm^{-1}	23.307	21.012
GOF on F^2	1.036	1.076
R_1[a] [$I>2\sigma(I)$]	0.0670	0.0820
wR_2[b] [$I>2\sigma(I)$]	0.1713	0.1995
R_1[a] (all data)	0.0791	0.1034
wR_2[b] (all data)	0.1827	0.2175

[a] $R_1 = \Sigma||F_o| - |F_c||/\Sigma|F_o|$. [b] $wR_2 = [\Sigma w(F_o^2 - F_c^2)^2/\Sigma w(F_o^2)^2]^{1/2}$; $w = 1/[\sigma^2(F_o^2) + (xP)^2 + yP]$, $P = (F_o^2 + 2F_c^2)/3$, where $x = 0.1402$, $y = 0.0000$ for **1** and $x = 0.1101$, $y = 127.6751$ for **2**.

Acknowledgments

This work was supported by the National Natural Science Fund for Distinguished Young Scholars of China (no. 20725101), the 973 Program (no. 2006CB932904), the NSF of Fujian Province (no. E0510030), the Knowledge Innovation Program of the Chinese Academy of Sciences (no. KJCX2.YW.H01), and the NFS of China (no. 20521101).

[1] a) M. T. Pope, *Heteropoly and Isopoly Oxometalates*, Springer, Berlin, **1983**; b) M. T. Pope, A. Müller (Eds.), *Polyoxometalates: From Platonic Solids to Anti-Retroviral Activity*, Kluwer, Dordrecht, The Netherlands, **1994**; c) M. T. Pope, A. Müller (Eds.), *Polyoxometalate Chemistry: From Topology via Self-Assembly to Applications*, Kluwer, Dordrecht, The Netherlands, **2001**.

[2] a) A. Müller, F. Peters, M. T. Pope, D. Gatteschi, *Chem. Rev.* **1998**, *98*, 239–272; b) C. L. Hill, *Comput. Coord. Chem. II* **2003**, *4*, 679–759; c) Y. G. Chen, J. Gong, L. Y. Qu, *Coord. Chem. Rev.* **2004**, *248*, 245–260.

[3] a) T. J. R. Weakley, H. T. Evans Jr., J. S. Showell, G. F. Tourné, C. M. Tourné, *J. Chem. Soc., Chem. Commun.* **1973**, 139–140; b) T. J. R. Weakley, R. G. Finke, *Inorg. Chem.* **1990**, *29*, 1235–1241; c) N. Casañ-Pastor, J. Bas-Serra, E. Coronado, G. Pourroy, L. C. W. Baker, *J. Am. Chem. Soc.* **1992**, *114*, 10380–10383; d) F. Xin, M. T. Pope, *J. Am. Chem. Soc.* **1996**, *118*, 7731–7736; e) M. Bösing, A. Nöh, I. Loose, B. Krebs, *J. Am. Chem. Soc.* **1998**, *120*, 7252–7259; f) J. M. Clemente-Juan, E. Coronado, J. R. Galán-Mascarós, C. J. Gómez-García, *Inorg. Chem.* **1999**, *38*, 55–63; g) S. Nellutla, J. van Tol, N. S. Dalal, L.-H. Bi, U. Kortz, B. Keita, L. Nadjo, G. A. Khitrov, A. G. Marshall, *Inorg. Chem.* **2005**, *44*, 9795–9806; h) Z. Zhang, Y. Li, E. Wang, X. Wang, C. Qin, H. An, *Inorg. Chem.* **2006**, *45*, 4313–4315.

[4] a) M. T. Pope, "Polyoxoanions: Synthesis and Structure" in *Comprehensive Coordination Chemistry II: Transition Metal Groups 3–6* (Ed.: A. G. Wedd), Elsevier Science, New York, **2004**, vol. 4, ch. 4.10, p. 635; b) J. J. Borrás-Almenar, E. Coronado, A. Müller, M. T. Pope (Eds.), *Polyoxometalate Molecular Science*, Kluwer, Dordrecht, The Netherlands, **2004**.

[5] I. M. Mbomekalle, B. Keita, M. Nierlich, U. Kortz, P. Berthet, L. Nadjo, *Inorg. Chem.* **2003**, *42*, 5143–5152.

[6] a) R. G. Finke, B. Rapko, T. J. R. Weakley, *Inorg. Chem.* **1989**, *28*, 1573–1579; b) U. Kortz, S. Isber, M. H. Dickman, D. Ravot, *Inorg. Chem.* **2000**, *39*, 2915–2922; c) U. Kortz, N. K. Al-Kassem, M. G. Savelieff, N. A. Al Kadi, M. Sadakane, *Inorg. Chem.* **2001**, *40*, 4742–4749; d) N. Laronze, J. Marrot, G. Hervé, *Inorg. Chem.* **2003**, *42*, 5857–5862; e) U. Kortz, S. Nellutla, A. C. Stowe, N. S. Dalal, U. Rauwald, W. Danquah, D. Ravot, *Inorg. Chem.* **2004**, *43*, 2308–2317; f) T. Yamase, K. Fukaya, H. Nojiri, Y. Ohshima, *Inorg. Chem.* **2006**, *45*, 7698–7704.

[7] a) D. Gatteschi, O. Kahn, J. S. Miller, F. Palacio (Eds.), *Magnetic Molecular Materials*, Kluwer, Dordrecht, The Netherlands, **1991**; b) D. Gatteschi, *Adv. Mater.* **1994**, *6*, 635–645; c) U. Kortz, Y. P. Jeannin, A. Tézé, G. Hervé, S. Isber, *Inorg. Chem.* **1999**, *38*, 3670–3675.

[8] C. J. Gómez-García, J. J. Almenar, E. Coronado, L. Ouahab, *Inorg. Chem.* **1994**, *33*, 4016–4022.

[9] L.-H. Bi, E.-B. Wang, J. Peng, R.-D. Huang, L. Xu, C.-W. Hu, *Inorg. Chem.* **2000**, *39*, 671–679.

[10] U. Kortz, I. M. Mbomekalle, B. Keita, L. Nadjo, P. Berthet, *Inorg. Chem.* **2002**, *41*, 6412–6416.

[11] U. Kortz, A. Tézé, G. Hervé, *Inorg. Chem.* **1999**, *38*, 2038–2042.

[12] B. Keita, E. Abdeljalil, L. Nadjo, R. Contant, R. Belghiche, *Electrochem. Commun.* **2001**, *3*, 56–62.

[13] a) S. Khanra, T. Weyhermuller, E. Rentschler, P. Chaudhuri, *Inorg. Chem.* **2005**, *44*, 8176–8178; b) V. Ovcharenko, E. Fursova, G. Romanenko, I. Eremenko, E. Tretyakov, V. Ikorskii, *Inorg. Chem.* **2006**, *45*, 5338–5350; c) M. Fondo, N. Ocampo, A. M. García-Deibe, R. Vicente, M. Corbella, M. R. Bermejo, J. Sanmartín, *Inorg. Chem.* **2006**, *45*, 255–262.

[14] a) S.-T. Zheng, D.-Q. Yuan, J. Zhang, H.-P. Jia, G.-Y. Yang, *Chem. Commun.* **2007**, 1858–1860; b) J.-W. Zhao, H.-P. Jia, J. Zhang, S.-T. Zheng, G.-Y. Yang, *Chem. Eur. J.* **2007**, *13*, 10030–10045; c) J.-W. Zhao, B. Li, S.-T. Zheng, G.-Y. Yang, *Cryst. Growth Des.* **2007**, *7*, 2658–2664; d) J.-W. Zhao, S.-T. Zheng, G.-Y. Yang, *J. Solid State Chem.* **2007**, *180*, 3317–3324; e) Z. Zhang, J. Liu, E. Wang, C. Qin, Y. Li, Y. Qi, X. Wang, *Dalton Trans.* **2008**, 463–468.
[15] S.-T. Zheng, D.-Q. Yuan, J. Zhang, G.-Y. Yang, *Inorg. Chem.* **2007**, *46*, 4569–4574.
[16] J.-W. Zhao, J. Zhang, S.-T. Zheng, G.-Y. Yang, *Chem. Commun.* **2008**, 570–572.
[17] a) R. A. Ludise, *Progress in Inorganic Chemistry*, Wiley Interscience, New York, **1962**, vol. 3; b) A. Rabenau, *Angew. Chem. Int. Ed. Engl.* **1985**, *24*, 1026–1040; c) R. A. Ludise, *Chem. Eng. News* **1987**, *65*, 30; d) P. J. Hagrman, D. Hagrman, J. Zubietua, *Angew. Chem. Int. Ed.* **1999**, *38*, 2638–2684; e) J. Gopalakrishnan, *Chem. Mater.* **1995**, *7*, 1265–1275.
[18] a) P. J. Domaille in *Inorganic Syntheses*, John Wiley & Sons, New York, **1990**, vol. 27, pp. 96–104; b) G. Hervé, A. Tézé, *Inorg. Chem.* **1977**, *16*, 2115–2117; c) Bi, L. H. Kortz, U. Nellutla, S. Stowe, A. C. van Tol, J. Dalal, N. S. Keita, B. L. Nadjo, *Inorg. Chem.* **2005**, *44*, 896–903; d) N. H. Nsouli, B. S. Bassil, M. H. Dickman, U. Kortz, B. Keita, L. Nadjo, *Inorg. Chem.* **2006**, *45*, 3858–3860; e) A. Tézé, G. Hervé in *Inorganic Syntheses*, John Wiley & Sons, New York, **1990**, vol. 27, pp. 85–96.
[19] G.-Y. Yang, S. C. Sevov, *Inorg. Chem.* **2001**, *40*, 2214–2215.
[20] I. D. Brown, D. Altermatt, *Acta Crystallogr., Sect. B* **1985**, *41*, 244–247.
[21] a) B. Godin, Y.-G. Chen, J. Vaissermann, L. Ruhlmann, M. Verdaguer, P. Gouzerh, *Angew. Chem. Int. Ed.* **2005**, *44*, 3072–3075; b) D.-L. Long, O. Brücher, C. Streb, L. Cronin, *Dalton Trans.* **2006**, 2852–2860; c) D.-L. Long, E. Burkholder, L. Cronin, *Chem. Soc. Rev.* **2007**, *36*, 105–121.
[22] N. Zamstein, A. Tarantul, B. Tsukerblat, *Inorg. Chem.* **2007**, *46*, 8851–8858.
[23] a) J. J. Borrás-Almenar, J. M. Clemente-Juan, E. Coronado, B. S. Tsukerblat, *Inorg. Chem.* **1999**, *38*, 6081–6088; b) J. J. Borrás-Almenar, J. M. Clemente-Juan, E. Coronado, B. S. Tsukerblat, *J. Comput. Chem.* **2001**, *22*, 985–991.
[24] a) P. Artus, C. Boskovic, J. Yoo, W. E. Streib, L.-C. Brunel, D. N. Hendrickson, G. Christou, *Inorg. Chem.* **2001**, *40*, 4199–4210; b) A. Forment-Aliaga, E. Coronado, M. Feliz, A. Gaita-Ariño, R. LIusar, F. M. Romero, *Inorg. Chem.* **2003**, *42*, 8019–8027; c) R. L. Carlin, *Magnetochemistry*, Springer, Berlin, **1986**.
[25] J. A. Bertrand, A. P. Ginsberg, R. I. Kaplan, K. C. Eirkwood, R. L. Martin, R. C. Sherwood, *Inorg. Chem.* **1971**, *10*, 240–246.
[26] a) G. M. Sheldrick, *SHELXS97: Program for Crystal Structure Solution*, University of Göttingen, Göttingen, Germany, **1997**; b) G. M. Sheldrick, *SHELXL97: Program for Crystal Structure Refinement*, University of Göttingen, Göttingen, Germany, **1997**.

Received: March 21, 2008
Published Online: July 10, 2008

